Available online at www.sciencedirect.com
ScienceDirect
Earth and Planetary Science Letters 257 (2007) 245–258
EPSL
www.elsevier.com/locate/epsl

Highly resolved Beryllium-10 record from ODP Site 1089—A global signal?

M. Christl [a,b,*], A. Mangini [a], P.W. Kubik [c]

[a] Heidelberger Akademie der Wissenschaften, Im Neuenheimer Feld 229, D-69120 Heidelberg, Germany
[b] Institute of Particle Physics, ETH Zurich, CH-8093 Zurich, Switzerland
[c] Paul Scherrer Institute c/o Institute of Particle Physics, ETH Zurich, CH-8093 Zurich, Switzerland

Received 22 August 2006; received in revised form 20 February 2007; accepted 20 February 2007
Available online 27 February 2007
Editor: M.L. Delaney

Abstract

In this study a highly resolved Beryllium-10-record from a rapidly accumulating sediment core located in the Southern Cape Basin (ODP Leg 177 Site 1089) is presented. To extract the global ^{10}Be-production signal from the sedimentary record a dedicated correction procedure is applied. First, sediment redistribution is quantified by applying Thorium-230-normalization, then lateral transport of ^{10}Be and ^{230}Th is assessed using simple box model calculations. The model results indicate that only minor transport corrections have to be applied. Thus, Site 1089 combines the advantage of good time resolution with nearly negligible oceanic transport of ^{10}Be leading to a favored site for the reconstruction of global ^{10}Be-production changes from marine sediments.

Our results suggest that the transport corrected ^{10}Be-record at Site 1089 reflects long-term variations of the global ^{10}Be-production rate over the past 300 kyr. The absolute values of the youngest (Holocene) samples are in good agreement with the estimated recent long-term averaged global ^{10}Be-production rate (deduced from observations). The variability of the ^{10}Be-flux over the past 300 kyr corresponds well to the expected range (deduced from model calculations). The comparison with other reconstructions of geomagnetic paleointensity and with records of cosmogenic nuclides further emphasizes the global character of this ^{10}Be-record. Therefore, our results show that it is possible to quantitatively extract the global ^{10}Be-production rate from a single marine record if transport processes are corrected for. Since the error of a single reconstruction is large a combination of several highly resolved and transport corrected ^{10}Be-records may lead to a significantly improved reconstruction of geomagnetic variability and of global cosmic ray flux and over the past 300 kyr.

Keywords: Beryllium-10; geomagnetic paleointensity; cosmogenic radionuclides; cosmic rays; Southern Ocean

1. Introduction

The production of cosmogenic radionuclides (e.g. ^{10}Be, ^{14}C or ^{36}Cl) on Earth is proportional to the flux of galactic cosmic rays (GCR) impinging on the upper atmosphere. The flux of GCR on Earth, in turn, is inversely related to the shielding strength of the solar induced interplanetary magnetic field (IMF) and the geomagnetic field [1]. Consequently, the atmospheric production of cosmogenic radionuclides depends on (i) the flux of GCR arriving at our solar system, (ii) the strength of the IMF, and (iii) the strength of the geomagnetic field. All of these parameters vary with time but on different time scales. While the flux of GCR

* Corresponding author. Institute of Particle Physics, HPK G23, Schafmattstrasse 20, CH-8093 Zurich, Switzerland.
E-mail address: christl@phys.ethz.ch (M. Christl).

0012-821X/$ - see front matter © 2007 Elsevier B.V. All rights reserved.
doi:10.1016/j.epsl.2007.02.035

reaching the solar system is expected to vary significantly on very long time scales (>100 Myr) [2], these variations are thought to be small [3] when compared to the other effects described in the following. During the Late Quaternary the IMF and the Earth's magnetic field showed several pronounced variations [4–7]. Records of geomagnetic paleointensity (GPI) show that the Earth's magnetic field varied on multi-centennial and longer time scales (e.g. [8,9]). Solar cycles of about 11, 87, and 210 yr are well known (e.g. [10,4,6]), but millennial variability of the sun has not unambiguously been detected (e.g. [11–14]). Consequently, it is generally assumed that geomagnetic modulation controls the millennial and even some centennial-scale variability of cosmogenic nuclide production while solar variability controls the production on shorter time scales.

The majority of ^{10}Be is produced in the stratosphere [1,15,16] and is quickly removed from the atmosphere by dry and wet precipitation (the atmospheric residence time is about 1 yr [17,18]). In the ocean, ^{10}Be adsorbs onto sinking particles and is slowly removed from the water column. Because of the long oceanic residence time (500–1000 yr [19,20]), periodic variations of the atmospheric ^{10}Be-production on decadal to multi-centennial time scales (mainly caused by solar variability) become strongly damped in the marine environment. Thus, ^{10}Be in marine sediments may be used to reconstruct production changes on long (multi-centennial and longer) time scales as attributed to the geomagnetic field. Moreover, possible long-term changes of the IMF (as suggested previously [12]) and changes in the GCR flux from outside the solar system would be recorded as well.

In the first part of this paper we focus on the transport of ^{10}Be in the marine environment. We estimate an allowed range within the ^{10}Be-flux that is expected to vary if it reflects long-term averaged ^{10}Be-production changes and we present a correction procedure to extract the production signal from a single marine sediment core. In the second part of the paper, the correction procedure is applied to reconstruct global ^{10}Be-production from ODP-Site 1089. To document the global character of the transport corrected ^{10}Be-record, it is compared to several globally significant records of GPI and to profiles of cosmogenic radionuclides in the final part of the paper.

2. Geomagnetic paleointensity and ^{10}Be in marine records

Many studies show a relationship between ^{10}Be and GPI in marine records (e.g. [21–25]). However, climate-induced variations are often much larger than the atmospheric production signal and it is still unclear whether (or to what extend) these records are influenced or overprinted by climate signals [26,27]. To estimate the so-called "allowed range" within the ^{10}Be-flux in deep-sea sediments is expected to vary if solely controlled by production changes, the long-term averaged (on centennial time scales) absolute value and relative range of the global ^{10}Be-production has to be assessed.

2.1. Relative variation of the long-term averaged global ^{10}Be-production

Model derived estimates (Fig. 1) show that the relative global ^{10}Be-production is expected to vary between about 0.6 and 1.9 [28] or between 0.7 and 2.1 [15] of its present value when the Earth's magnetic field changes from zero to more than twice its recent field strength reflecting the observed variability during the Quaternary [7] (calculated under the assumption of constant mean solar activity). Due to the long oceanic residence time of ^{10}Be both, spatial inhomogeneities (e.g. latitude-dependency) and short-term variability (e.g. solar modulation) of atmospheric ^{10}Be-production are expected to be averaged. Consequently, in this study we assume that the relative variation of the long-term averaged global ^{10}Be-production ranges between 0.65 and 2.0 of its present value reflecting the mean range predicted by the simulations [28,15].

2.2. Absolute value of the long-term averaged global ^{10}Be-production

Both, model calculations [1,15,29,16] and observations (see Monaghan et al. [30] and references therein) show very different estimates for the absolute value of

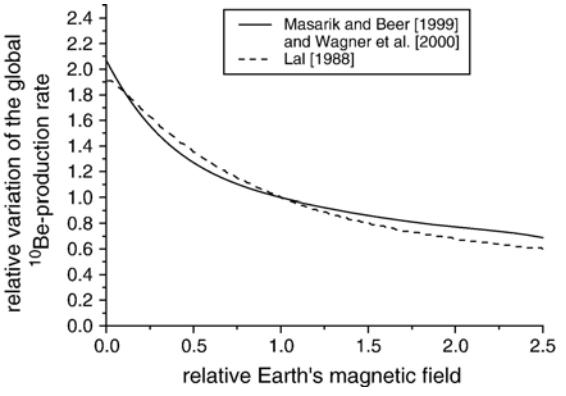

Fig. 1. Two different model estimates of the relative variation of the global ^{10}Be-production rate as a function of the Earth's magnetic field strength under the assumption of mean solar magnetic activity given by Lal [28] (dashed line) and Masarik and Beer [15] (straight line; the polynomial equation is presented by Wagner et al. [64]).

the recent global ^{10}Be-production rate. While models still have to deal with large uncertainties in the absolute values of the nuclear cross sections for the different reactions producing ^{10}Be, observations of ^{10}Be-deposition in various archives apparently are strongly influenced by the complex distribution and scavenging behavior of ^{10}Be in the troposphere. In this study we use a recent global ^{10}Be-production rate of $(1.21\pm0.26)\times 10^6$ at cm^{-2} yr^{-1} [30] calculated from precipitation samples continuously collected during 1980. This value is corrected for the latitude dependency of the ^{10}Be-supply to the Earth's surface and it is corrected for recycled ^{10}Be derived by the suspension and deposition of soil particles. However, it cannot directly be assigned to marine sediments because it is a 1-yr, not a centennial average. In 1979/80 (the residence time of ^{10}Be in the atmosphere is about 1 yr) the 11 yr sunspot-cycle showed a maximum indicating increased IMF-strength, which caused a lower global ^{10}Be-production compared to the long-term average. Following the model estimates [1,15], the global production rate of ^{10}Be during solar maximum is 15–16% lower compared to the average over a complete solar cycle. Consequently, the 11 yr averaged global ^{10}Be-production rate based on the value measured in 1980 [30] is assessed to be $(1.4\pm0.3)\times10^6$ at cm^{-2} yr^{-1}. On centennial time scales, the geomagnetic aa-index (available since 1868) generally is used as a proxy for solar magnetic activity (e.g. [31,32]). The mean aa-index in 1979/80 was (20.5±2.8) nT, very close to the long-term average of (19.3±6) nT measured between 1868 and 2000. Therefore we assume that the production rate of $(1.4\pm0.3)\times10^6$ at cm^{-2} yr^{-1} calculated above already reflects the long-term (centennial) averaged value of global ^{10}Be-production as it is recorded in marine sediments. By combining the above results the allowed range of the ^{10}Be-flux into marine sediments or any other archive recording globally integrated and long-term averaged production changes is estimated to vary between $0.65\times(1.4\times10^9)=0.9\times10^9$ at cm^{-2} kyr^{-1} and $2.0\times(1.4\times10^9)=2.8\times10^9$ at cm^{-2} kyr^{-1}. Although the uncertainty of this estimation is large (22% for each threshold, estimated from the error in the global production rate and the different values for the relative range given by the models), it provides a simple tool (a necessary condition) to check whether a marine ^{10}Be-record reflects geomagnetic variability or whether it is influenced by climate related signals.

3. Site description

ODP Leg 177, Site 1089 is located in the southeastern South Atlantic at the northern flank of the Agulhas Ridge in the southern Cape Basin (40°56′S, 9°53′E) at a water depth of 4621 m [33]. Hydrographically it is situated in the northern part of the eastward flowing Antarctic Circumpolar Current (ACC) south of the Subtropical Front, which bounds the ACC to the north. On glacial to interglacial time scale deep and bottom water flow at Site 1089 is linked to global conveyor circulation [34]. Presently, Site 1089 is bathed in Circumpolar Deep Water (CPDW) that has similar physical and chemical properties compared to Pacific water masses entering the South Atlantic via the Drake Passage. Site 1089 shows a pacific like carbonate preservation pattern (high carbonate glacials and low-carbonate interglacials) reflecting changes in the saturation state of deep and bottom water masses in the deep Cape Basin [35]. Due to its location on a drift deposit, Site 1089 shows continuously high sedimentation rates (about 15 cm/kyr, Fig. 2a) over the last 580 kyr [35,36]

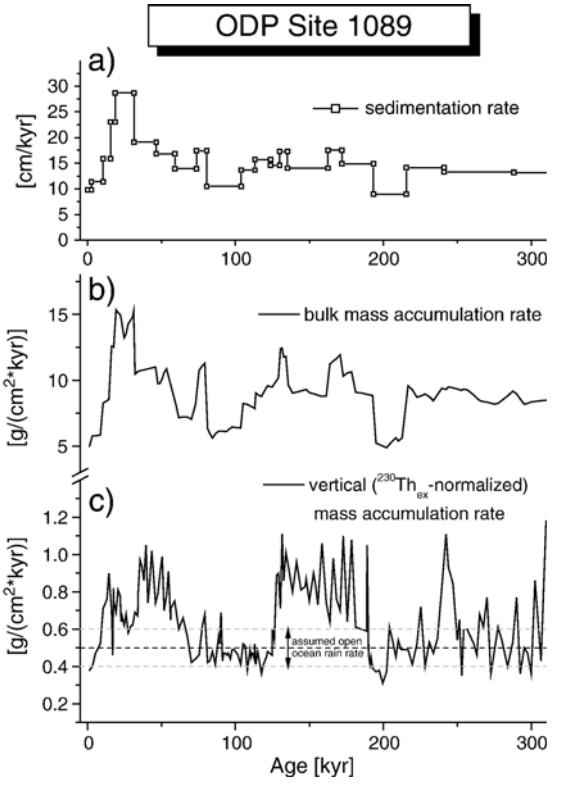

Fig. 2. (a) Sedimentation rate [36], (b) bulk mass accumulation rate and (c) vertical (^{230}Th$_{ex}$-normalized) mass accumulation rate (c) at ODP Site 1089 over the past 300 kyr. The curve in (c) is identical to the correction term in Eq. (1) ($\beta\cdot z/^{230}$Th$_{ex}$) that is used to calculate the ^{230}Th$_{ex}$-normalized ^{10}Be-flux (see also Section 5.2.1). The dashed lines in (c) show the assumed open ocean rain rate used for the model calculations. The vertical arrow indicates the respective error range.

permitting a good time resolution for paleoclimate studies on millennial to sub-millennial time scales. Therefore, Site 1089 provides the high resolution Southern Hemisphere analog to the drift deposits from the North Atlantic Ocean drilled during Legs 162 and 172.

4. Age model and accumulation rates

The age model of Site 1089 was derived by mapping the benthic and planktic foraminiferal $\delta^{18}O$-data to the SPECMAP stack over the past 580 kyr [37]. The age model is further constrained by correlating Site 1089 isotope data to those from adjacent core RC11-83 that has 14 radiocarbon ages in the 11-41 kyr interval and to a benthic record from core 21-PC02 [37,36]. Over the past 300 kyr, sedimentation rates (Fig. 2a) as well as mass accumulation rates (Fig. 2b) are high, ranging between 5 and 32 cm kyr^{-1} and 5 and 15 g cm^{-2} kyr^{-1}, respectively. Vertical (Th-normalized) accumulation rates (Fig. 2c, see also Section 5.2.1) are comparable to open ocean values indicating that Site 1089 is affected by strong sediment focusing and most probably was not located in a biologically active high particle flux area over the past 300 kyr.

5. Methods

5.1. Sample preparation and measurement

In this study $^{230}Th_{ex}$-normalized ^{10}Be-fluxes from ODP Site 1089 are presented. For this purpose, sediment samples were analyzed for thorium and uranium isotopes, and for their ^{10}Be-content. Chemical preparation of the Th/U-samples followed standard procedures (e.g. [38]). The measurements of ^{230}Th, ^{232}Th, ^{238}U and ^{234}U activities were performed by alpha counting. The analytical error of the alpha-measurements mostly ranges between 5% and 8% reaching values of more than 10% for certain samples with very low activities or low chemical yield. Chemical separation of ^{10}Be for accelerator mass spectrometry (AMS) also followed previously described methods (e.g. [23]). The purified ^{10}Be-samples were co-precipitated with silver to avoid grinding and mixing the Be-oxide with copper powder (adopted from Stone et al., [39]). ^{10}Be-measurements were conducted at the AMS-facility of Paul Scherrer Institute and ETH Zurich, Switzerland. The typical analytical error of the AMS measurement was 3–5%. The measured ratios were normalized to the internal standard S555 with a nominal $^{10}Be/^{9}Be$-ratio of 95.5×10^{-12}. Measured ^{10}Be-concentrations were decay corrected using a half-life of 1.52 Myr [40].

5.2. Transport corrections

To extract the ^{10}Be-production signal from marine sediments two major oceanic transport processes have to be considered (atmospheric transport can be neglected because the ocean is considered as well mixed due to the long oceanic residence time of Be). First, dissolved ^{10}Be may be transported laterally by advection or eddy diffusion and can be deposited preferentially in biologically active high particle flux areas (i.e. enhanced scavenging, e.g. [19]). Second, once-deposited ^{10}Be can be redistributed with the sediments, for example by bottom currents, and then be re-deposited elsewhere (i.e. sediment focusing/winnowing, e.g. [41]). Over the last years, considerable progress has been made to understand the transport of ^{10}Be in the ocean. A constant-flux-tracer normalization-procedure to correct for sediment redistribution was established [42,41] and ocean models simulating the distribution of dissolved ^{230}Th and ^{10}Be to correct for enhanced scavenging were used [43–45]. Alternative normalizing techniques have been developed to extract only the authigenic (stemming from the sea water) $^{10}Be/^{9}Be$-ratio from deep sea sediments [46,47,27]. Although first results using the authigenic $^{10}Be/^{9}Be$-ratio are promising [47,48] a direct comparison with the well established and widely applied $^{230}Th_{ex}$-normalization technique has not been presented yet. The ^{10}Be-record presented in this study is successively corrected for sediment redistribution and for enhanced scavenging using dedicated techniques described in the following.

5.2.1. $^{230}Th_{ex}$-normalization

The $^{230}Th_{ex}$-normalization method is applied to calculate vertical ^{10}Be-fluxes (rain rates). Because ^{230}Th is the most widely applied constant flux proxy for marine sediments deposited during the Late Quaternary [42] this method is briefly described here (for further details see e.g. [42,41,49–52]). According to this technique the vertical flux of any sedimentary component can be calculated as:

$$F_i = C_i \cdot \frac{\beta \cdot z}{^{230}\mathrm{Th}^{0}_{\mathrm{ex}}} \quad (1)$$

Where F_i is the vertical flux of component i, C_i is the concentration of (i) in the sediment, $\beta \cdot z$ is the production rate of ^{230}Th in the water column ($\beta = 2.63\times10^{-5}$ dpm cm^{-3} kyr^{-1}, z = water depth [cm]), and $^{230}Th^{0}_{ex}$ is the decay corrected specific $^{230}Th_{ex}$-activity [dpm/g]. Note, that Eq. (1) only depends on the measured concentration of the sedimentary component (here the measured and

decay corrected ^{10}Be-concentration) and the specific $^{230}Th^{0}_{ex}$-activity.

Recently, the $^{230}Th_{ex}$-profiling method became a topic of controversial discussion [53]. By using geophysical seismic data the authors found that the $^{230}Th_{ex}$-profiling technique probably overestimates sediment focusing in the equatorial Pacific by a factor of 10 to 20. This deviation was attributed to post depositional transport effects of ^{230}Th ("leakage" of ^{230}Th from the sea floor and advection of re-adsorbed ^{230}Th with fine grained particles). However, by comparing the ^{230}Th-activity with grain size distribution in the terrigenous fraction [34] no indications for a post depositional transport of ^{230}Th are found at Site 1089 (R^2=0.012, not shown here). Therefore, we conclude that the $^{230}Th_{ex}$-profiling method can be applied successfully at Site 1089 and that it provides a robust tool to quantify sediment focusing and to calculate $^{230}Th_{ex}$-normalized ^{10}Be-fluxes.

5.2.2. Enhanced scavenging

To correct the $^{230}Th_{ex}$-normalized ^{10}Be-record for enhanced scavenging simple box model calculations are applied. The identical two-box model was used previously to correct already existing $^{230}Th_{ex}$-normalized ^{10}Be-records for enhanced scavenging of ^{10}Be. A detailed model description is given in [44]. In this study, the South Atlantic type parameter set (Section 2.3 in [44]) is used. The only time-dependent input variable for the model calculations is the $^{230}Th_{ex}$-derived vertical mass accumulation rate of the corresponding sediment core (Fig. 2c). As a constant model parameter, the open ocean rain rate has to be defined. In this study, a vertical mass accumulation rate (MAR) of (0.5±0.1) g cm^{-2} kyr^{-1} is assumed (dashed lines in Fig. 2c) representing the mean accumulation rate in the open Atlantic Ocean. This value is consistent with earlier simulations [44] and it takes into account that Site 1089 is a drift deposit accumulating sediments deposited in open ocean areas. To assess the dependency of the calculated correction factors on the choice of the open ocean rain rate, it was varied by ±20% (0.4–0.6 g cm^{-2} kyr^{-1}). An additional error of 10% was estimated that has to be added to the final transport corrected ^{10}Be-record. Based on the above input values, the ^{10}Be-Scavenging Factor (^{10}Be-SCF, Eq. (1) in [44]), depicting how much more ^{10}Be compared to ^{230}Th is imported (SCF>1) or exported (SCF<1) at a certain location is calculated. To derive the final transport corrected ^{10}Be-record, the $^{230}Th_{ex}$-normalized ^{10}Be-flux has to be divided by the modeled scavenging factors (applied in Section 6.1).

6. Geomagnetic paleointensity and transport corrected ^{10}Be-flux at Site 1089

6.1. ^{10}Be-record at Site 1089

The measured ^{10}Be-concentration (Fig. 3a, open circles) strongly correlates with (the inversed) carbonate content (red dotted line in Fig. 3a) at ODP Site 1089. Over the past about 600 kyr the carbonate content is strongly influenced by variable dissolution/preservation caused by different mixtures of Pacific with Atlantic deep water masses in the abyssal Cape Basin [37,35]. Because the carbonate concentration at Site 1089 is controlled by climate, the ^{10}Be-concentration, in turn, simply reflects this (climate related) carbonate preservation pattern and therefore is not related to ^{10}Be-production changes or geomagnetic variability at all. Because variable carbonate preservation, influence of different water masses, changing bioproductivity, sediment redistribution, etc. are common features of marine sedimentary records the measured ^{10}Be-concentration (even if carbonate corrected) generally cannot be used as a proxy for GPI. Instead, the depositional flux of ^{10}Be is not influenced by dissolution of carbonate and changes in (vertical) sedimentation rate (e.g. [54]). However, the (bulk) depositional flux of ^{10}Be calculated as the product of total sedimentation rate, ^{10}Be-concentration and dry bulk density may be strongly influenced by sediment redistribution (e.g. [42]). Syndepositional focusing in particular affects drift deposits like Site 1089, and the $^{230}Th_{ex}$-data suggest that lateral sediment import over the past 300 kyr was on average about 16 times larger than the vertical supply at Site 1089. The average total flux of ^{10}Be was about 30×10^9 at cm^{-2} kyr^{-1} over the past 300 kyr, which is more than 20 times the recent long-term averaged global ^{10}Be-production rate, and which apparently was caused by sediment focusing, not by geomagnetic variability. To correct for sediment focusing, $^{230}Th_{ex}$-normalized vertical ^{10}Be-accumulation rates were calculated using Eq. (1) (Fig. 3b, solid line with open circles). There are two strong indicators that the $^{230}Th_{ex}$-normalized ^{10}Be-record at Site 1089 already reflects changes in the global ^{10}Be-production rate (as it would be expected if ^{10}Be behaves as an ideal conservative tracer in the Southern Ocean, [55]). First, the three youngest samples are close to the estimated recent long-term averaged global production rate of 1.4×10^9 at cm^{-2} kyr^{-1} (horizontal, dashed line in Fig. 3b). Second, the two most prominent ^{10}Be-peaks (Fig. 3b) correspond to two well-known paleomagnetic minima, the Laschamp Event at around 40 kyr and the Jamaica Event at about 190 kyr. A ^{10}Be-

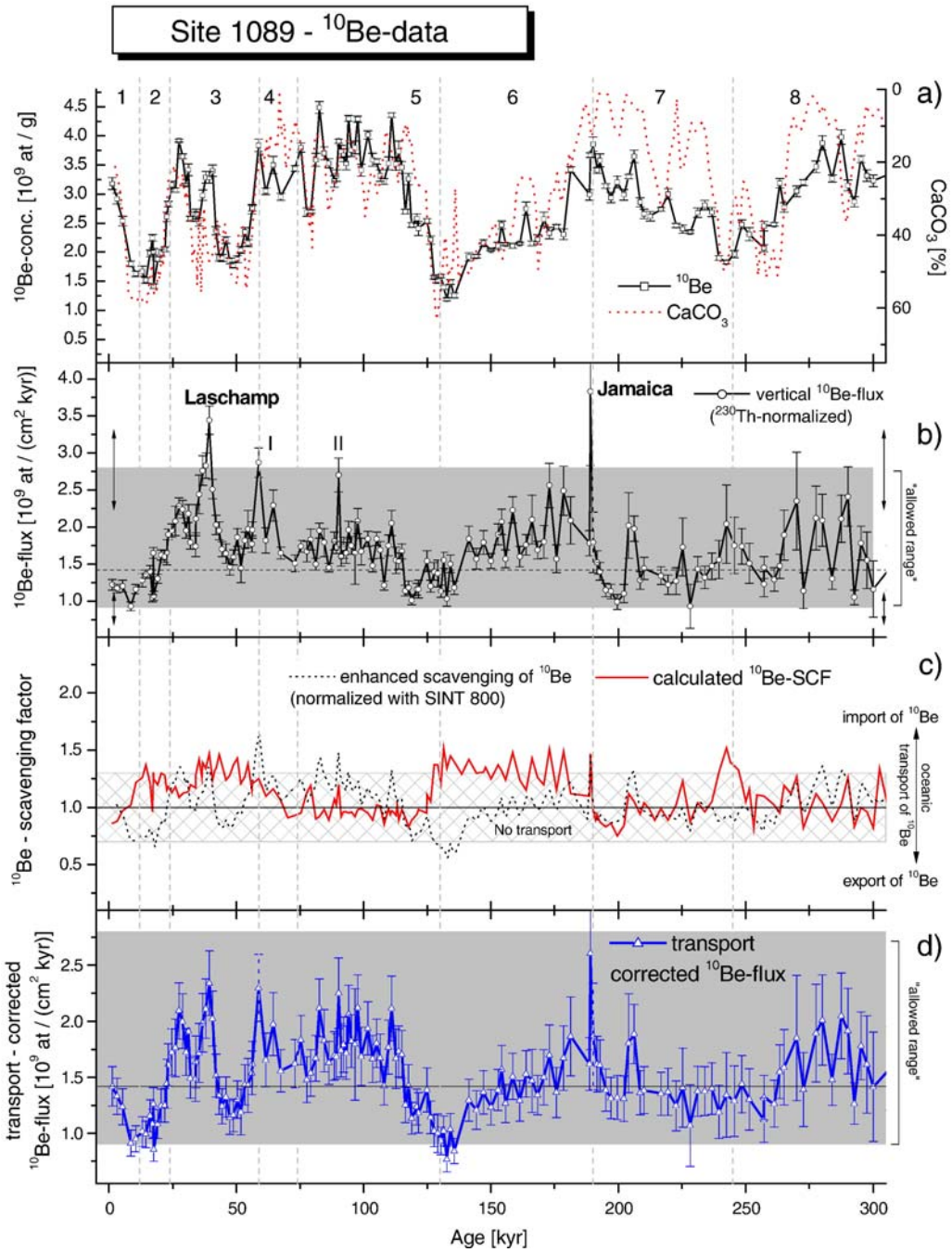

Fig. 3. The numbers and dashed vertical lines in this and the following plots indicate the Marine Isotope Stages (MIS 1–8) and their boundaries, respectively. (a) Measured and decay corrected ^{10}Be-concentration (black line, open squares) over the past 300 kyr compared to the climatically controlled (inverse) $CaCO_3$-concentration (red dotted line) at Site 1089. (b) $^{230}Th_{ex}$-normalized flux of ^{10}Be at Site 1089 (vertical accumulation rate) over the past 300 kyr (black line, open circles). Relative maxima in the ^{10}Be-flux coincide with the Laschamp Event (40 kyr) and the Jamaica Event (about 190 kyr). The 60-kyr and the 90-kyr peaks are labeled I and II. The horizontal line marks the estimated recent long-term averaged global ^{10}Be-production-rate. The gray area indicates the estimated allowed range (see text for details) together with its uncertainty (vertical arrows). (c) SINT-normalized (black dashed line) and modeled ^{10}Be-SCF (red line) at Site 1089. A ^{10}Be-SCF above the hatched area ('no transport' area) indicates an import of ^{10}Be while ^{10}Be-SCF below this area reflects an export of ^{10}Be to adjacent open ocean areas (see text for details). The modeled correction factors (red line) are used to correct the $^{230}Th_{ex}$-normalized record for enhanced scavenging of ^{10}Be. (d) Transport corrected ^{10}Be-flux at Site 1089 over the past 300 kyr (blue line, open triangles). The gray area again indicates the allowed range. The horizontal line reflects the estimated recent long-term averaged global ^{10}Be-productioin-rate.

peak at 60 kyr (I in Fig. 3b) also was observed in the Vostok ice core [56], but the peak around 90 kyr (II in Fig. 3b) seems to occur too late to be associated with the Blake Event. The fact that it will be almost removed by the subsequent transport correction further suggests that this peak probably was not caused by a geomagnetic event. We note that the error of the Jamaica-peak is large making it difficult to determine its true height, but we see a clear increasing trend in the ^{10}Be-flux from about 200 to 190 kyr, which we interpret as the Jamaica peak. Consequently, 3 out of 4 relative maxima of the $^{230}Th_{ex}$-normalized ^{10}Be-flux (although caused by only a few data points) can be related to geomagnetic events or have been observed in other (ice core) ^{10}Be-records. Although the variation of the $^{230}Th_{ex}$-normalized ^{10}Be-flux is relatively large (more than a factor of 3), within the uncertainty of the estimated limits this record is consistent with the allowed range defined above (gray area in Fig. 3b). Nevertheless, it is very likely that a small climate induced signal still is present in the $^{230}Th_{ex}$-normalized record (e.g. [44,26]). For example, $^{230}Th_{ex}$-normalized ^{10}Be-records have been used successfully to reconstruct Late Quaternary particle fluxes in the Southern Ocean (enhanced scavenging is assumed to be proportional to particle flux) [57,58]. In particular, a $^{230}Th_{ex}$-normalized ^{10}Be-record additionally corrected of for changes in GPI was used to arrive at a purely particle flux related signal [57]. To estimate the influence of enhanced scavenging at Site 1089 we divided the $^{230}Th_{ex}$-normalized ^{10}Be-record by the ^{10}Be-production changes expected from the SINT 800 data (using the polynomial function plotted in Fig. 1 [64] and the absolute value of ^{10}Be-production estimated above). The resulting record (black dashed line in Fig. 3c) is very similar to the ^{10}Be-SCF described in Section 5.2.2. However, it may be influenced by offsets in the age models of the individual records, and it may overestimate enhanced scavenging of Be because this approach does not account for the possible transport of Th. In general, the transport of Th compared to Be is considered to be small [59,45,60], so that the SINT-normalized record of enhanced scavenging (black dashed line in Fig. 3c) should be comparable with the modeled ^{10}Be-SCF (Section 5.2.2) at Site 1089 (red line in Fig. 3c). Both (independently derived) estimates of enhanced scavenging show similar variability over the past 300 kyr. The SINT-normalized record of enhanced scavenging (as expected) shows larger variations compared with the modeled^{10}Be-SCF. Major deviations between both records of enhanced scavenging (in particular around 45 and 130 kyr) may be removed by aligning the individual chronologies of the SINT-record and Site 1089 (see also Fig. 5a). Despite the above discrepancies, both, the modeled ^{10}Be-SCF and the SINT-normalized reconstruction of enhanced scavenging do not deviate much from the 'no-transport' area (hatched region in Fig. 3c with ^{10}Be-SCFs around 1±30% error range estimated from the uncertainty of ^{10}Be-production rate (about 20%) and the uncertainty of $^{230}Th_{ex}$-normalization (up to 25% [42]) indicating that most of the time none or very little additional transport of ^{10}Be influenced the $^{230}Th_{ex}$-normalized ^{10}Be-flux at Site 1089. Based on this result we conclude that the $^{230}Th_{ex}$-normalized ^{10}Be-deposition rate already is a good proxy for the reconstruction of global ^{10}Be-production rate and for GPI at Site 1089.

To eliminate the small residual transport signal that potentially is present in the data, the $^{230}Th_{ex}$-normalized ^{10}Be-record (Fig. 3b) is divided by the modeled correction factors (red dotted line in Fig. 3c). Due to the uncertainty of the model calculations (Section 5.2.2), an additional error of 10% is added to the resulting transport corrected ^{10}Be-record (Fig. 3d, in all following figures plotted as blue line with open triangles). The transport corrected ^{10}Be-record now is corrected for sediment focusing and for enhanced scavenging. Therefore, it should mainly represent variations of the long-term averaged global ^{10}Be-production rate over the past 300 kyr. All data points plot within the allowed range (gray area in Fig. 3d), and the youngest samples match the estimated recent long-term averaged global production rate (dashed line in Fig. 3d) very well. The Laschamp Event (40 kyr) and the Jamaica Event (190 kyr) are still the most prominent peaks in the record, and the 28-kyr peak (probably the so-called Mono Lake) as well as the 60-kyr peak (Vostok) have become more pronounced in the transport corrected record. The broad maximum in the ^{10}Be-flux around 100 kyr accompanied by several short ^{10}Be-peaks make it difficult to identify the Blake Event in this record. A broad ^{10}Be-peak around the Blake Event also has been found in previous studies (e.g. [22]).

6.2. Global character of the ^{10}Be-record

To show the global character of the transport corrected ^{10}Be-flux at Site 1089 it is compared to magnetization data from the same site, to the highly resolved Northern Hemisphere NAPIS-record, and to the global SINT 800 record. Furthermore it is compared to records of cosmogenic nuclides from different archives. All records are plotted on their own time scale no tuning or wiggle matching was applied.

6.2.1. The last 75 kyr

Over the past about 75 kyr high-resolution paleointensity and cosmogenic records exist. For comparison

with the ^{10}Be-flux at Site 1089 we selected two paleointensity records, three different reconstructions of atmospheric Δ^{14}C, and a highly resolved ^{10}Be-record (Fig. 4). When compared with GPI-records the ^{10}Be-flux always is plotted on a logarithmic scale, because the production of ^{10}Be is not linearly related with GPI (Fig. 1). This sufficiently accounts for the higher sensitivity of ^{10}Be-production to low dipole strengths (maximal deviation compared to the original relation in Fig. 1 is about 10%).

First, the transport corrected ^{10}Be-flux at Site 1089 is compared to the (inverse scaled) paleointensity record from the same site (Fig. 4a), and to the NAPIS record (Fig. 4b). We note that the magnetization signal at Site 1089 is affected by post depositional diagenetic transformations seriously constraining the applicability of the magnetization signal at Site 1089 as a GPI-proxy [36]. Despite the known limitations of the magnetization data it is compared to the ^{10}Be-record from the same site because both records are not affected by any error in the chronology. The NAPIS record, therefore, reflects the more global reconstruction of GPI compared to Site 1089. Although time resolution of the ^{10}Be-flux is much poorer compared to the GPI-data, it tends to match the both GPI-records quite well. Three ^{10}Be-peaks (around 30, 40, and 60 kyr) can be found in the NAPIS-record (relative minima) and to a lesser extend in the GPI-record from Site 1089. Between about 60 and 30 kyr Site 1089 GPI seems to be shifted by about 1000 to 1500 yr to older ages when compared to the ^{10}Be-flux. Based on the residence time of Be it is expected that the ^{10}Be-signal lags the magnetization signal by some hundreds of years. The additional shift may have been caused by an inadequate correction of the lock-in depth between 30 and 60 kyr. Due to the limited reliability of the magnetization data this is not further discussed. Note that a possible time-shift (caused by both, the variable lock in depth and the residence time of Be) has to be considered if highly resolved ^{10}Be- and GPI-records are used to synchronize chronologies.

Second, the ^{10}Be-flux at Site 1089 is compared to several reconstructions of atmospheric Δ^{14}C from different archives (Fig. 4c). We are aware of the potential problems when comparing ^{10}Be-flux with Δ^{14}C. To correctly compare the records the ^{10}Be-data have to be converted into a Δ^{14}C-record. For such model calculations (spanning glacial/interglacial time scales) assumptions about the global carbon cycle, and about ocean circulation have to be made that are speculative. Moreover, model studies were not able to reproduce the measured atmospheric Δ^{14}C values over the past 50 kyr within the established limits for carbon cycle and ocean circulation [61,62]. Because of the above limitations this comparison has to be considered qualitatively only. Except for the Δ^{14}C peak around 44 kyr that is solely observed in the stalagmite record there is a reasonable (qualitative) correlation of the different radiocarbon records with the ^{10}Be-flux at Site 1089 (Fig. 4c). While the marine reconstructions of Δ^{14}C seem to match with the ^{10}Be-flux between about 60 and 25 kyr, deviations occur in the younger part of the record. We note that, although the best match is observed with the stalagmite-based reconstruction of atmospheric Δ^{14}C, the variability of this record, however, is much higher than explainable by geomagnetic field changes during the period older than 35 kyr. As discussed above, this comparison may only be used as a qualitative indicator to show that the ^{10}Be-record at Site 1089 is controlled by global production changes.

Finally, the transport corrected ^{10}Be-record is compared to the ^{10}Be-flux to the Summit ice cores (GISP2, GRIP) in Greenland over the past 60 kyr [63] (Fig. 4d, gray line: unfiltered data, black line: smoothed data). The ice core record shows a pronounced Laschamp Event around 40 kyr, and between about 30 and 60 kyr the marine and the ice core record corresponds fairly well. However, discrepancies occur for samples younger than 30 kyr. Between 30 and 20 kyr the ^{10}Be-flux at Site 1089 matches better to the NAPIS record (Fig. 4b) than to the Summit^{10}Be-record, while the situation is inversed during the past about 20 kyr (Fig. 4d). The absolute values of ^{10}Be-deposition at Summit do not fit in the allowed range estimated above. The flux at Summit ranges between 0.3 and 0.6×10^{9} at cm^{-2} kyr^{-1}, which is only 20–40% of the estimated recent long-term averaged global ^{10}Be-production rate and which is only 20–40% of the average ^{10}Be-flux at Site 1089. This deviation seems to be too large to be explained by uncertainties in the global ^{10}Be-production rate suggesting that the ^{10}Be-flux at Summit reflects only a certain part of the globally integrated and long-term averaged signal. In contrast, several studies have successfully extracted geomagnetic and solar variability from Greenland ice cores (e.g. [10,63,6,64]) suggesting that the relatively small ^{10}Be-flux at Summit (compared to the estimated long-term averaged global ^{10}Be-flux) reflects a fixed part (constant over time) of the globally integrated ^{10}Be-production which is not very sensitive to climate induced transport as previously suggested [65].

6.2.2. The last 300 kyr

To document the global character of the whole 300 kyr period, the ^{10}Be-record from Site 1089 is compared to the SINT 800-stack [66] (Fig. 5a), to the

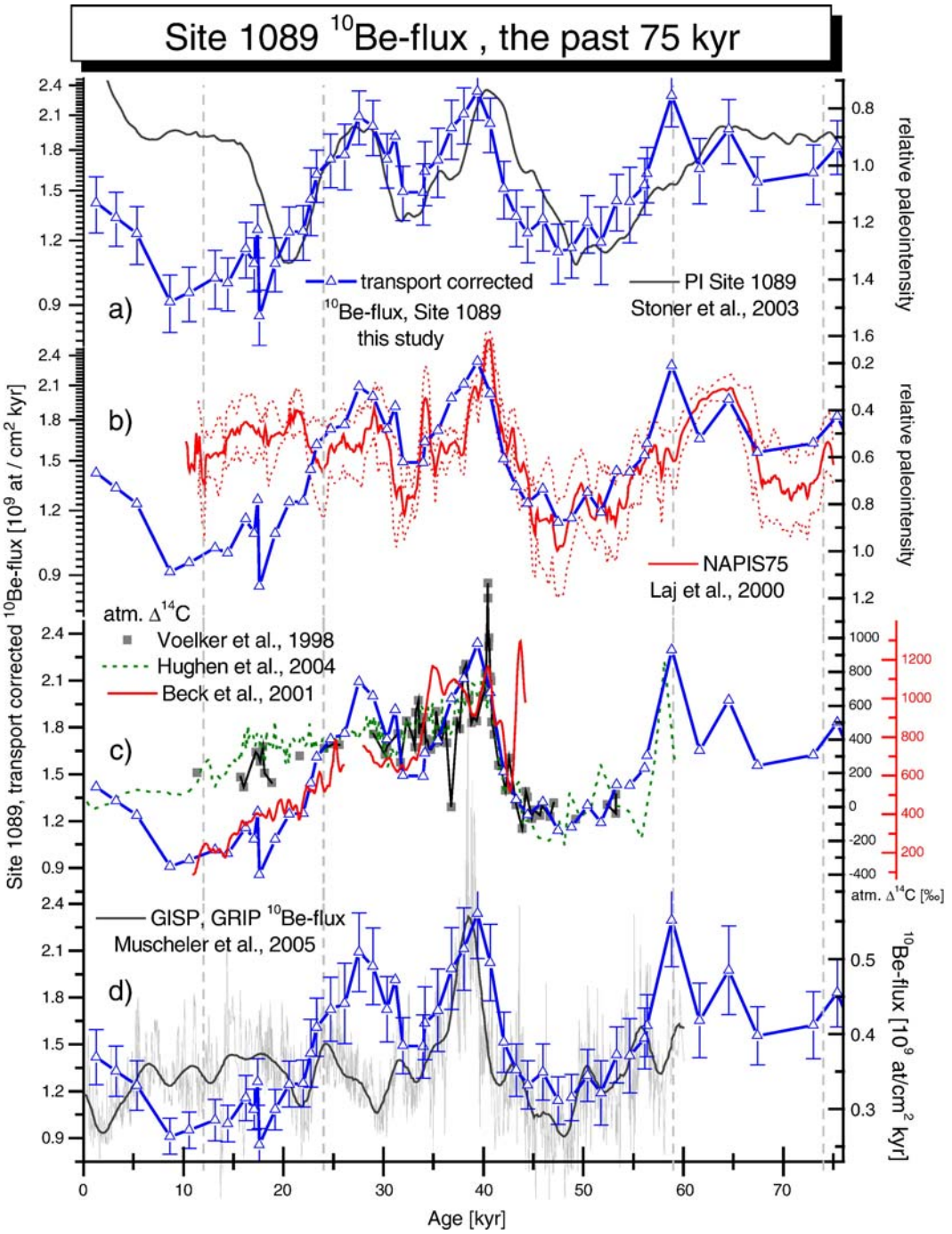

Fig. 4. ^{10}Be-flux at Site 1089 over the past 75 kyr. The transport corrected ^{10}Be-record (blue line, open triangles) is plotted on the same scale in all diagrams. For comparison with paleointensity records a logarithmic scale type is used (see text for details). All records are plotted on their own chronologies. (a) ^{10}Be-flux and GPI (smoothed data, black line) from the same site (ODP Site 1089). Note that the geomagnetic record from Site 1089 is not an ideal proxy for GPI (see text). (b) ^{10}Be-flux at Site 1089 compared to the high-resolution NAPIS-75 stack [68] (red line), the error range of the NAPIS-record is indicated by the red dotted line. (c) The ^{10}Be-flux at Site 1089 is (qualitatively) compared to different reconstructions of atmospheric Δ^{14}C: from a marine sediment core located north of Iceland [69] (gray filled squares, black line), based on ^{14}C data from Cariaco Basin sediments [61] (green dotted line), and based on a stalagmite recovered from a submerged cave in the Bahamas [70] (red line). A good qualitative correlation is observed with the Δ^{14}C reconstructed from a submerged stalagmite. However, this Δ^{14}C signal (red scale) cannot be explained by geomagnetic variability alone. (d) ^{10}Be-flux recorded at Summit (GISP2, GRIP ice cores, [63]) compared to Site 1089 (smoothed data: black line, original data: small gray line).

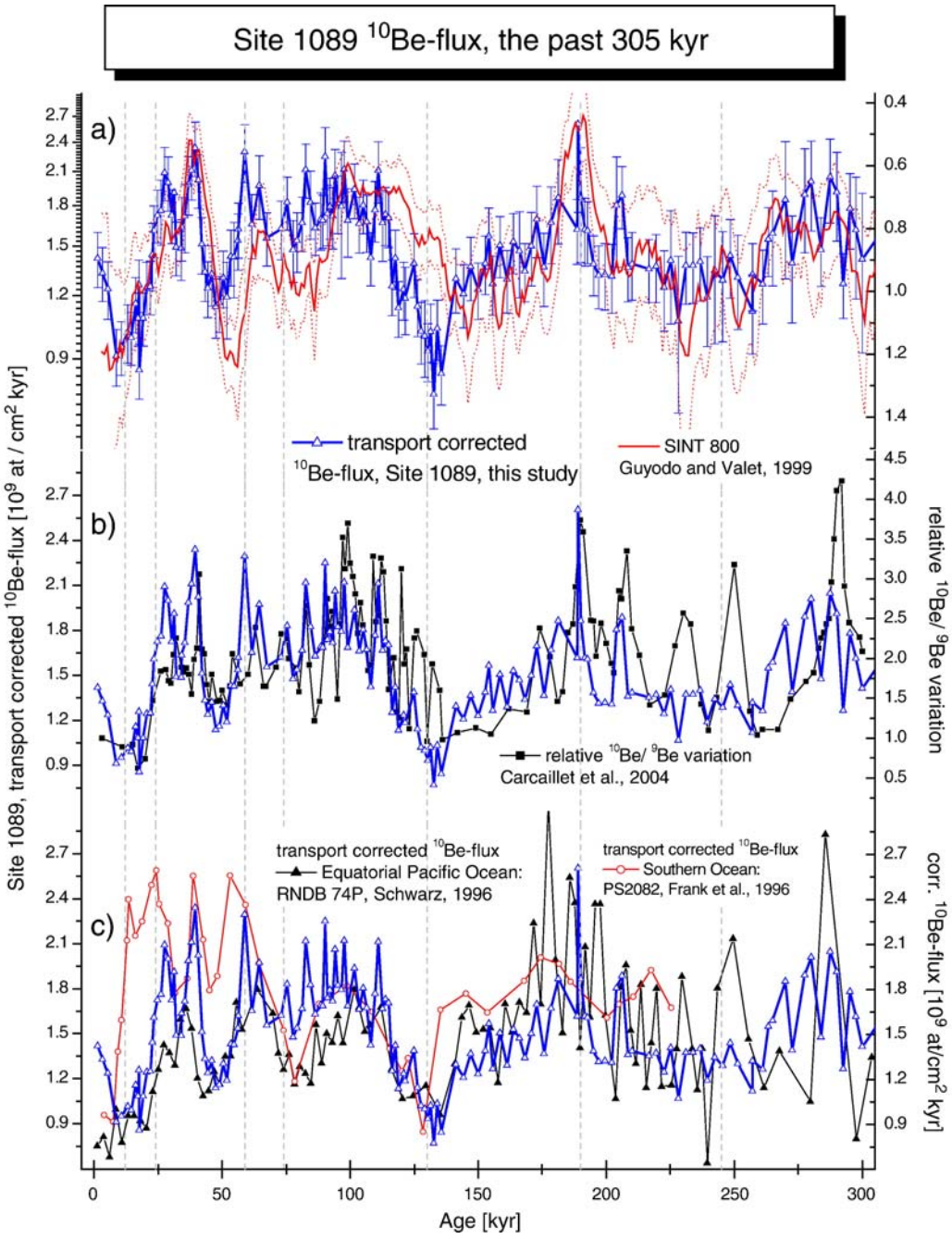

Fig. 5. ^{10}Be-flux at Site 1089 over the past 305 kyr. The transport corrected ^{10}Be-record (blue line, open triangles) is plotted on the same scale in all diagrams. For comparison with paleointensity records a logarithmic scale type is used. All records are plotted on their own chronologies. (a) The ^{10}Be-flux at Site 1089 is compared to the globally stacked SINT 800 record (red line), the error range of the SINT-record is indicated by the red dotted line [66]. The correlation could be improved by adjusting the age models of both records. (b) ^{10}Be-flux at Site 1089 and the relative variation of the authigenic ^{10}Be/^{9}Be-ratio (black line with filled squares) off the coast of Portugal [47]. Note that the variability of the authigenic ^{10}Be/^{9}Be-ratio is larger than expected from geomagnetic dipole changes. (c) The transport corrected flux of ^{10}Be in different ocean basins and different sedimentary regimes: Site 1089: highly accumulating South Atlantic drift deposit; PS2082: nearby Site 1089, but about 250 km closer to the Polar Frontal Zone, located in the Agulhas Basin [67] (red line with open circles); RNDB 74P: slowly accumulating open Pacific record [54] from the Ontong Java Plateau (black line with filled triangles) [44,54] (see text for further discussion).

relative variation of the authigenic $^{10}Be/^{9}Be$-ratio off the coast of Portugal [47] (Fig. 5b), and to different transport corrected ($^{230}Th_{ex}$-normalized and model corrected) ^{10}Be-records in the Equatorial Pacific Ocean and in the Southern Ocean [44,67,54] (Fig. 5c).

A good (anti-) correlation of ^{10}Be-flux at Site 1089 with the SINT 800-record is observed over the past 300 kyr (Fig. 5a). The correlation obviously can be improved by adjusting the time scales of the two records. However, the offset between about 115 and 140 kyr seems too large (about 8–10 kyr) to be explained by dating uncertainties of the different records, a variable lock in depth of the magnetization signal, the residence time of ^{10}Be in the ocean, or by a combination of all three effects. An unexplained deviation between a stacked ^{10}Be-record and the SINT-curve during approximately the same age range has been reported earlier [44,22]. The authors speculated that perhaps the sampling of cores with a uniformly reduced local ^{10}Be-rain rate during that time could have biased their results. Although this explanation cannot be completely excluded for Site 1089, modeled ^{10}Be-SCF does not indicate an unusually high export of ^{10}Be during this time (Fig. 5c). Thus, the deviation between cosmogenic ^{10}Be and the SINT-record between 115 and 140 kyr remains unexplained in this study.

Second, the ^{10}Be-flux at Site 1089 is compared to the relative variation of the authigenic $^{10}Be/^{9}Be$-ratio off the coast of Portugal [47] (Fig. 5b). The records show a very similar pattern indicating that both reflect changes of global ^{10}Be-production. However, the variability of the authigenic $^{10}Be/^{9}Be$-ratio (factor of 4) is much larger than expected from the geomagnetic variation suggesting that this record not solely reflects ^{10}Be-production changes. In particular between 200 and 300 kyr the variability of the authigenic $^{10}Be/^{9}Be$-ratio is much larger than (i) the transport corrected ^{10}Be-flux at Site 1089, and (ii) the estimated range due to geomagnetic variability.

Finally, Site 1089 ^{10}Be-record is compared to two $^{230}Th_{ex}$-normalized and transport corrected ^{10}Be-records from different ocean basins (Fig. 5c). All records are plotted on the same scale. Despite their location in very different sedimentary regimes (Site 1089: highly accumulating South Atlantic drift deposit; PS2082: nearby Site 1089, but about 250 km closer to the Polar Frontal Zone, located in the Agulhas Basin [67]; RNDB 74P: slowly accumulating open Pacific record [54] from the Ontong Java Plateau), the transport corrected records show very similar variability and absolute values of ^{10}Be-deposition over the whole age range. All transport corrected marine ^{10}Be-records plot within the allowed range (except for four data points of record RNDB 74P). Given that the error range of each single record is up to 20% (not shown for better visibility), it is difficult to discuss the differences within individual records in detail, but some systematic deviations seem to occur. For example, between about 300 and 170 kyr the ^{10}Be-flux in the Equatorial Pacific shows a larger variability than at Site 1089, whereas the ^{10}Be-record from PS2082 deviates systematically from Site 1089 during parts of the last Glacial (MIS 2 and 3). These deviations may be related to improper corrections caused by the simplified box model or may be caused by additional processes not accounted for by the model calculations (e.g. additional ^{10}Be transported by melt waters, or changes in ocean circulation). For example, a constant correction factor was applied to quantify the export of ^{10}Be to adjacent high particle flux regions for the Pacific record [44]. However, it is very likely that Site RNDB74P was influenced by a more variable transport signal causing the observed short-term fluctuations of ^{10}Be-accumulation (exceeding the 'allowed' range given above) between 300 and 170 kyr. The potential influence of ocean circulation (e.g. glacial weakening of Thermohaline Circulation) causing a larger proportion of glacial Pacific deep waters with higher ^{10}Be-concentrations entering the Southern Ocean has been suggested to explain the unexpected high ^{10}Be-deposition rates at site PS2082 during MIS 2 and 3 [44]. Furthermore, a contribution of ^{10}Be from iceberg melting, in particular in the area around the Polar Front, where a large quantity of icebergs melt and at the same time and particulate scavenging is high, could not be excluded in a previous study [55]. Record PS 2082 (closest to the Polar Front) indeed shows highest deposition rates during the last Glacial (MIS 2 and 3). Site 1089 probably is less influenced by additional ^{10}Be transported by melt waters because the drift sediments originate from further North and represent a more basin-wide average (mixture between proximal and distal sources) than at site PS2082. The variability of ^{10}Be-rich glacial pacific deep waters also is expected to be smaller because (^{10}Be-rich) Pacific-type waters (with variable mixtures of North Atlantic-type waters) formed the main source of bottom waters at Site 1089 over the past about 600 kyr [37].

7. Conclusions

The application of a dedicated correction procedure enabled us to extract the global ^{10}Be-production rate from a highly accumulating marine sediment core (ODP Leg 177 Site 1089, Southern Cape Basin). First, the ^{10}Be-data were $^{230}Th_{ex}$-normalized to correct for sediment redistribution. Then, simple box model calculations were used to

quantify the lateral transport of ^{230}Th and ^{10}Be. Our results suggest that the transport corrected ^{10}Be-flux at Site 1089 reflects the globally integrated and long-term averaged atmospheric ^{10}Be-production rate over the past 300 kyr, which is inversely related to the geomagnetic dipole strength. This evidence is based on the following results/observations: (i) The transport corrected ^{10}Be-flux at Site 1089 shows distinct peaks that can be linked to global geomagnetic events. (ii) The youngest (Holocene) samples match the estimated recent long-term averaged global ^{10}Be-production rate very well. (iii) The transport corrected ^{10}Be-flux at Site 1089 plots within the allowed range that can be explained by geomagnetic dipole changes. (iv) There is a good qualitative correlation with other reconstructions of GPI and with different globally significant records of cosmogenic nuclides from polar ice cores and marine archives.

Our results, therefore, show that it is possible to quantitatively extract the global ^{10}Be-production signal from a single marine record. Although the error of a single reconstruction is large, the combination of several highly resolved and transport corrected ^{10}Be-records may be used to construct a global marine ^{10}Be-stack leading to a significantly improved reconstruction of GPI from ^{10}Be in marine sediments. Such a record, for example, can be used as a tool to match marine, terrestrial, and ice core chronologies on the millennial and probably the sub-millennial time scale or it may serve as an indicator for the global GCR-flux over the past 300 kyr.

Acknowledgement

This study was granted by the Deutsche Forschungsgemeinschaft (DFG Projects CH386/1 and CH386/2). M.C. currently is funded by CRONUS-EU. We want to thank: IODP and the people from the Bremen core repository for their excellent service providing the samples and additional leg-related information; the “HiWis” in the Heidelberg geochemistry lab for preparing numerous samples; the Zurich AMS-team for their support during the ^{10}Be-measurments; B. Schulze and J. Lippold for their comments. We appreciate the discussions with J. Beer and we want to thank the reviewers (M. Frank, R. Muscheler, and M. Sharma) and the Editor (P. Delaney) for their helpful and constructive comments substantially improving the quality of this paper.

References

[1] D. Lal, B. Peters, Cosmic ray produced radioactivity on the Earth, Handbook of Physics, Springer, 1967, pp. 551–612.

[2] N.J. Shaviv, The spiral structure of the Milky Way, cosmic rays, and ice age epochs on Earth, New Astron. 8 (1) (2003) 39–77.

[3] S. Vogt, G.F. Herzog, R.C. Reedy, Cosmogenic nuclides in extraterrestrial materials, Rev. Geophys. 28 (1990) 253–275.

[4] A.N. Peristykh, P.E. Damon, Persistence of the Gleissberg 88-year solar cycle over the last ~12,000 years: evidence from cosmogenic isotopes, J. Geophys. Res., [Space Phys.] 108 (A1) (2003) 1003.

[5] J.-P. Valet, L. Meynadier, Y. Guyodo, Geomagnetic dipole strength and reversal rate over the past two million years, Nature 435 (2005) 802–805.

[6] G. Wagner, et al., Presence of the solar de Vries cycle (similar to 205 years) during the last ice age, Geophys. Res. Lett. 28 (2) (2001) 303–306.

[7] T. Yamazaki, H. Oda, Orbital influence on Earth’s magnetic field: 100,000-year periodicity in inclination, Science 295 (5564) (2002) 2435–2438.

[8] G. St-Onge, J.S. Stoner, C. Hillaire-Marcel, The effect of magnetic anisotropy on paleomagnetic directions in high-grade metamorphic rocks from the Juiz de Fora Complex, SE Brazil, Earth Planet. Sci. Lett. 209 (1-2) (2003) 113–130.

[9] S. Yang, H. Odah, J. Shaw, Variations in the geomagnetic dipole moment over the last 12000 years, Geophys. J. Int. 140 (1) (2000) 158–162.

[10] J. Beer, J. Blinov, G. Bonani, H.J. Hofmann, R.C. Finkel, Use of Be-10 in polar ice to trace the 11-year cycle of solar activity, Nature 347 (1990) 164–166.

[11] E. Bard, M. Frank, Climate change and solar variability: what’s new under the sun? Earth Planet. Sci. Lett. 248 (1-2) (2006) 1–14.

[12] M. Sharma, Variations in solar magnetic activity during the last 200,000 years: is there a Sun-climate connection? Earth Planet. Sci. Lett. 199 (3-4) (2002) 459–472.

[13] M. Stuiver, T.F. Braziunas, Sun, ocean, climate and atmospheric $^{14}CO_2$: an evaluation of causal and spectral relationships, Holocene 3 (4) (1993) 289–305.

[14] M. Stuiver, T.F. Braziunas, B. Becker, B. Kromer, Climatic, solar, oceanic, and geomagnetic influences on late-glacial and Holocene atmospheric $^{14}C/^{12}C$ change, Quat. Res. 35 (1) (1991) 1–24.

[15] J. Masarik, J. Beer, Simulation of particle fluxes and cosmogenic nuclide production in the Earth’s atmosphere, J. Geophys. Res., [Atmos.] 104 (D10) (1999) 12099–12111.

[16] K. O’Brien, Secular variations in the production of cosmogenic isotopes in the Earth’s atmosphere, J. Geophys. Res. 84 (1979) 423–431.

[17] L.R. McHargue, P.E. Damon, The global beryllium-10 cycle, Rev. Geophys. 29 (2) (1991) 141–158.

[18] G.M. Raisbeck, et al., Be-10 in the environment: some recent results and their application, Symposium of Accelerator Mass Spectrometry III, Argonne Natl. Lab, Argonne, 1981, p. 458.

[19] R.F. Anderson, et al., Boundary scavenging in the Pacific Ocean: a comparison of ^{10}Be and ^{231}Pa, Earth Planet. Sci. Lett. 96 (3-4) (1990) 287–304.

[20] T.L. Ku, et al., Beryllium isotope distribution in the western North Atlantic: a comparison to the Pacific, Deep-Sea Res. 37 (5A) (1990) 795–808.

[21] A. Aldahan, G. Possnert, The Be-10 marine record of the last 3.5 Ma, Nucl. Instrum. Methods Phys. Res., B Beam Interact. Mater. Atoms 172 (2000) 513–517.

[22] M. Frank, et al., A 200 kyr record of cosmogenic radionuclide production rate and geomagnetic field intensity from Be-10 in globally stacked deep-sea sediments, Earth Planet. Sci. Lett. 149 (1-4) (1997) 121–129.

[23] W.U. Henken-Mellies, et al., ^{10}Be and ^{9}Be in South Atlantic DSDP Site 519; relation to geomagnetic reversals and to sediment composition, Earth Planet. Sci. Lett. 98 (3-4) (1990) 267–276.
[24] L.R. McHargue, et al., Geomagnetic modulation of the late Pleistocene cosmic-ray flux as determined by Be-10 from Blake Outer Ridge marine sediments, Nucl. Instrum. Methods Phys. Res., B Beam Interact. Mater. Atoms 172 (2000) 555–561.
[25] G.M. Raisbeck, F. Yiou, A search in a marine sediment core for Be-10 concentration variations during a geomagnetic field reversal, Geophys. Res. Lett. 6 (9) (1979) 717–719.
[26] Y.S. Kok, Climatic influence in NRM and Be-10-derived geomagnetic paleointensity data, Earth Planet. Sci. Lett. 166 (3-4) (1999) 105–119.
[27] L.R. McHargue, D.J. Donahue, Effects of climate and the cosmic-ray flux on the ^{10}Be content of marine sediments, Earth Planet. Sci. Lett. 232 (1-2) (2005) 193–207.
[28] D. Lal, Theoretically expected variations in the terrestrial cosmic-ray production rates of isotopes, Soc. Italiana di Fisica-Bologna-Italy XCV corso, 1988, pp. 216–233.
[29] J. Masarik, R.C. Reedy, Terrestrial cosmogenic-nuclide production systematics calculated from numerical simulations, Earth Planet. Sci. Lett. 136 (3-4) (1995) 381–395.
[30] M.C. Monaghan, S. Krishnaswami, K.K. Turekian, The global-average production rate of ^{10}Be, Earth Planet. Sci. Lett. 76 (3-4) (1986) 279–287.
[31] M. Lockwood, R. Stamper, M.N. Wild, A doubling of the Sun's coronal magnetic field during the past 100 years, Nature 399 (6735) (1999) 437–439.
[32] R. Stamper, M. Lockwood, M.N. Wild, T.D.G. Clark, Solar causes of the long-term increase in geomagnetic activity, J. Geophys. Res., [Space Phys.] 104 (A12) (1999) 28325–28342.
[33] Gersonde, R., Hodell, D.A., Blum, P., 1999. Proc. ODP, Init. Repts., 177 [CD-ROM], Ocean Drilling Program. Texas A & M University, College Station, TX 77845-9547, U.S.A.
[34] G. Kuhn, B. Diekmann, Late Quaternary variability of ocean circulation in the southeastern South Atlantic inferred from the terrigenous sediment record of a drift deposit in the southern Cape Basin (ODP Site 1089), Palaeogeogr. Palaeoclimatol. Palaeoecol. 182 (2002) 287–333.
[35] D.A. Hodell, R. Gersonde, P. Blum, Leg 177 synthesis: insights into Southern Ocean paleoceanography on tectonic to millennial timescales, in: R. Gersonde, D.A. Hodell, P. Blum (Eds.), Proc. ODP, Sci. Results, vol. 177, 2002, http://www-odp.tamu.edu/publications/177_SR/synth/synth.htm.
[36] J.S. Stoner, J.E.T. Channell, D.A. Hodell, C.D. Charles, A ~580 kyr paleomagnetic record from the sub-Antarctic South Atlantic (Ocean Drilling Program Site 1089), J. Geophys. Res. 108 (B5) (2003) 2244.
[37] D.A. Hodell, C.D. Charles, F.J. Sierro, Late Pleistocene evolution of the ocean's carbonate system, Earth Planet. Sci. Lett. 192 (2) (2001) 109–124.
[38] M. Frank, et al., Beryllium 10, thorium 230, and protactinium 231 in Galapagos microplate sediments: implications of hydrothermal activity and paleoproductivity changes during the last 100 000 years, Paleoceanography 9 (4) (1994) 559–578.
[39] J. Stone, et al., Co-precipitated silver-metal oxide aggregates for accelerator mass spectrometry of ^{10}Be and ^{26}Al, Nuclear Instruments and Methods in Physics Research Section B: Beam Interactions with Materials and Atoms, Proceedings of the Ninth International Conference on Accelerator Mass Spectrometry, vol. 223-224, 2004, pp. 272–277.
[40] H.J. Hofmann, et al., ^{10}Be half-life and AMS-standards, Nucl. Instrum. Methods Phys. Res., B Beam Interact. Mater. Atoms B29 (1987) 2–36.
[41] M. Frank, R. Gersonde, A. Mangini, Sediment redistribution, ^{230}Thex-normalization and implications for the reconstruction of particle flux and export paleoproductivity, in: G. Fischer, G. Wefer (Eds.), Use of Proxies in Paleoceanography: Examples from the South Atlantic, Springer-Verlag, New York, 1999, pp. 409–426.
[42] R. Francois, M. Frank, M.M. Rutgers van der Loeff, M.P. Bacon, ^{230}Th-normalization: an essential tool for interpreting sedimentary fluxes during the late Quaternary, Paleoceanography 19 (1) (2004) 16.
[43] M. Christl, S. Siegle, C. Strobl, S. Reuter, A. Mangini, Distribution and Sedimentary flux of ^{10}Be, ^{230}Th and ^{231}Pa in the South Atlantic Ocean on a glacial/interglacial timescale; a multibox model approach, Geochim. Cosmochim. Acta 66 (15A) (2002) A141.
[44] M. Christl, C. Strobl, A. Mangini, Beryllium-10 in deep-sea sediments: a tracer for the Earth's magnetic field intensity during the last 200,000 years, Quat. Sci. Rev. 22 (5-7) (2003) 725–739.
[45] G.M. Henderson, C. Heinze, R.F. Anderson, A.M.E. Winguth, Global distribution of the Th-230 flux to ocean sediments constrained by GCM modelling, Deep-Sea Res., Part 1, Oceanogr. Res. Pap. 46 (11) (1999) 1861–1893.
[46] D. Bourles, G.M. Raisbeck, F. Yiou, ^{10}Be and ^{9}Be in marine sediments and their potential for dating, Geochim. Cosmochim. Acta 53 (2) (1989) 443–452.
[47] J. Carcaillet, D.L. Bourles, N. Thouveny, M. Arnold, A high resolution authigenic ^{10}Be/^{9}Be record of geomagnetic moment variations over the last 300 ka from sedimentary cores of the Portuguese margin, Earth Planet. Sci. Lett. 219 (3-4) (2004) 397–412.
[48] G. Leduc, N. Thouveny, D.L. Bourles, C.L. Blanchet, J.T. Carcaillet, Authigenic ^{10}Be/^{9}Be signature of the Laschamp excursion: a tool for global synchronisation of paleoclimatic archives, Earth Planet. Sci. Lett. 245 (1-2) (2006) 19–28.
[49] M.P. Bacon, Glacial to interglacial changes in carbonate and clay sedimentation in the Atlantic Ocean estimated from ^{230}Th measurements, Chem. Geol. 46 (2) (1984) 97–111.
[50] J.K. Cochran, J.K. Osmond, Sedimentation patterns and accumulation rates in the Tasman Basin, Deep-Sea Res. 23 (1) (1976) 193–210.
[51] R. Francois, M.P. Bacon, D.O. Suman, Thorium-230 in deep sea sediments: high resolution records of flux and dissolution of carbonate in the Equatorial Atlantic during the last 24,000 years, Paleoceanography 5 (5) (1990) 761–787.
[52] F. Marcantonio, et al., Sediment focusing in the central equatorial Pacific Ocean, Paleoceanography 16 (3) (2001) 260–267.
[53] M. Lyle, N. Mitchell, N.G. Pisias, A. Mix, J.I. Martinez, Do geochemical estimates of sediment focusing pass the sediment test in the equatorial Pacific? Paleoceanography 20 (1) (2005) 1–12.
[54] Schwarz, B., Mangini, A., Segl, M., 1996. Geochemistry of a piston core from Ontong Java Plateau (western equatorial Pacific); evidence for sediment redistribution and changes in paleoproductivity. In: Anonymous (Editor), Global change and marine geology. Geologische Rundschau. Springer International, Berlin, Federal Republic of Germany, pp. 536-545.
[55] M. Frank, M.M. Rutgers van der Loeff, P.W. Kubik, A. Mangini, Quasi-conservative behaviour of ^{10}Be in deep waters of the Weddell Sea and the Atlantic sector of the Antarctic Circumpolar Current, Earth Planet. Sci. Lett. 201 (1) (2002) 171–186.
[56] G.M. Raisbeck, et al., Evidence for two intervals of enhanced ^{10}Be deposition in Antarctic ice during the last glacial period, Nature 326 (6110) (1987) 273–277.

[57] M. Frank, et al., Similar glacial and interglacial export bioproductivity in the Atlantic sector of the Southern Ocean: multiproxy evidence and implications for glacial atmospheric CO_2, Paleoceanography 15 (6) (2000) 642–658.
[58] N. Kumar, et al., Increased biological productivity and export production in the glacial Southern Ocean, Nature 378 (6558) (1995) 675–680.
[59] R.F. Anderson, M.P. Bacon, P.G. Brewer, Removal of ^{230}Th and ^{231}Pa from the open ocean, Earth Planet. Sci. Lett. 62 (1) (1983) 7–23.
[60] N. Kumar, R. Gwiazda, R.F. Anderson, P.N. Froelich, ^{231}Pa/^{230}Th ratios in sediments as a proxy for past changes in Southern Ocean productivity, Nature (Lond.) 362 (6415) (1993) 45–48.
[61] K. Hughen, et al., ^{14}C activity and global carbon cycle changes over the past 50,000 years, Science 303 (5655) (2004) 202–207.
[62] C. Laj, et al., Geomagnetic field intensity, North Atlantic Deep Water circulation and atmospheric Delta C-14 during the last 50 kyr, Earth Planet. Sci. Lett. 200 (1-2) (2002) 177–190.
[63] R. Muscheler, J. Beer, P.W. Kubik, H.-A. Synal, Geomagnetic field intensity during the last 60,000 years based on ^{10}Be and ^{36}Cl from the summit ice cores and ^{14}C, Quat. Sci. Rev. 24 (16-17) (2005) 1849–1860.
[64] G. Wagner, et al., Reconstruction of the geomagnetic field between 20 and 60 kyr BP from cosmogenic radionuclides in the GRIP ice core, Nucl. Instrum. Methods Phys. Res., B Beam Interact. Mater. Atoms 172 (2000) 597–604.
[65] C.V. Field, G.A. Schmidt, D. Koch, C. Salyk, Modeling production and climate-related impacts on ^{10}Be concentration in ice cores, J. Geophys. Res. 111 (2006) D15107.
[66] Y. Guyodo, J.P. Valet, Global changes in intensity of the Earth's magnetic field during the past 800 kyr, Nature 399 (6733) (1999) 249–252.
[67] M. Frank, Reconstruction of Late Quaternary Environmental Conditions Applying the Natural Radionuclides ^{230}Th, ^{10}Be, ^{231}Pa and ^{238}U: A Study of Deep-Sea Sediments from the Eastern Sector of the Antarctic Circumpolar Current System, Alfred Wegner Institute for Polar and Marine Research, 1996.
[68] C. Laj, C. Kissel, A. Mazaud, J.E.T. Channell, J. Beer, North Atlantic palaeointensity stack since 75 ka (NAPIS-75) and the duration of the Laschamp event, Philos. Trans. R. Soc. Lond. Ser. A: Math. Phys. Eng. Sci. 358 (1768) (2000) 1009–1025.
[69] A. Voelker, et al., Correlation of marine ^{14}C ages from the Nordic Seas with the GISP2 isotopic record: implications for radiocarbon calibration beyond 25 ka BP, Radiocarbon 40 (1) (1998) 517–534.
[70] J.W. Beck, et al., Extremely large variations of atmospheric ^{14}C concentration during the last glacial period, Science 292 (5526) (2001) 2453–2458.